INTERNATIONAL JOURNAL OF GEOMAGNETISM AND AERONOMY
VOL. 3, NO. 2, PAGES 141–150, DECEMBER 2002

Acceleration and heating in the auroral magnetosphere by current-driven electrostatic ion-cyclotron turbulence

V. E. Zakharov

Department of Physics, Kaliningrad State University, Russia

C.-V. Meister

Potsdam Astrophysical Institute, Germany

Abstract. A numerical magnetohydrodynamic (MHD) model is developed to investigate acceleration and heating of both thermal and auroral plasma. This is done for magnetospheric flux tubes in which intensive field-aligned currents flow. For each of these tubes, the empirical Tsyganenko model of the magnetospheric field is used. The parameters of the background plasma outside the flux tube as well as the strength of the electric field of magnetospheric convection are given. Performing the numerical calculations, the distributions of the plasma densities, velocities, temperatures, parallel electric field and current, and of the coefficients of thermal conductivity are obtained in a self-consistent way. It is found that electrostatic ion-cyclotron (EIC) turbulence develops effectively in the thermal plasma. The parallel electric field develops under the action of the anomalous resistivity. This electric field accelerates both the thermal and auroral plasma. The thermal turbulent plasma is also subjected to intensive heating. The increase of the plasma temperature strongly depends on the value of the magnetic flux in the given tube and on the intensity of the magnetospheric convection. It is found that even stationary EIC turbulence may cause large-scale resistivity of the plasma of Earth's ionosphere. Besides studying the growth and dispersion properties of oblique ion-cyclotron waves excited in a drifting magnetized plasma, it is shown that under non-stationary conditions, such waves may reveal the properties of bursts of polarized transverse electromagnetic waves at frequencies near the proton gyrofrequency.

1. Introduction

As known, both the magnetic field and the plasma of the magnetosphere are non-uniform. The pressure gradients of the plasma are caused by the electromotive force that produces electric currents in the magnetosphere. The ionosphere is the resistivity load connected to the magnetospheric sources of electric power via highly conducting magnetic field lines. The magnetospheric and ionospheric current system is closed by the field-aligned electric currents (FAC).

Kindel and Kennel [1971] suggested that electrostatic ion-cyclotron (EIC) waves could be produced by FAC. The EIC waves are usually found in regions with upgoing ion beams [*André et al.*, 1987]. EIC waves have spectral peaks above the ion gyrofrequencies and sometimes at higher harmonics.

Waves also may be essential for the formation of a quasi-static difference of the electric potential V along the magnetic field lines. Microinstabilities cause anomalous resistivity in the plasma and the appearance of the electric fields $\mathbf{E}_{\|}$

Paper number GAI01376.
CCC: 1524–4423/2002/0302–0376$18.00

The online version of this paper was published 9 December 2002.
URL: http://ijga.agu.org/v03/gai01376/gai01376.htm
Print companion issued December 2002.

parallel to **B** [*Lysak and Dum*, 1983]. A second generation mechanism of these fields is based on a local charge separation in the FAC regions, where electrostatic double layers occur [*Block*, 1975; *Block and Fälthammar*, 1991]. Both generation mechanisms do not exclude one another; instead, they complement one another. *Hesse et al.* [1990] considered both mechanisms, applying the resistive fluid theory to the field-aligned potential structures.

Auroral arcs may be present because the parallel electric fields accelerate the auroral electrons downward [*Chiu and Cornwall*, 1980]. Strong electric spikes of about 100 mV m^{-1} were locally detected by the Freja satellite [*Chust et al.*, 1988]. Using the results of observations obtained by polar orbiting satellites, it was shown that the potential differences are usually located at altitudes between 2000 and 15,000 km [*Reiff et al.*, 1988, 1993]. *Reiff et al.* [1993] also estimated that the potential differences may be as large as $\Delta V \approx 1 - 10$ kV. At the same altitudes, perpendicular spatial scales of about 100 km are most typical for the parallel electric fields [*Gorney*, 1984]. Besides, finer scales have been observed inside the larger features.

The electric component of the electromagnetic waves, if it is parallel to the geomagnetic field **B**, modulates the field-aligned fluxes of the electrons at the wave frequency. In the case of electromagnetic ion-cyclotron (EMIC) waves, the modulation effect has been detected by sounding rockets [*Lund and LaBelle*, 1997; *Temerin et al.*, 1993]. *Erlandson et al.* [1994] observed the EMIC waves by Freja satellite in a region of inverted V-type electron precipitation. Using simultaneous Freja observations of precipitating keV electrons and EMIC waves, *Oscarsson et al.* [1997] concluded that the EMIC wave-particle interaction is resonant at altitudes of several thousands of kilometers above the auroral ionosphere.

Growth and damping of the oblique EMIC waves were studied by *Xue et al.* [1996] for the conditions of the Earth's outer magnetosphere ($L = 7$, where L is the geomagnetic shell parameter) when the energetic particle distribution has a high-energy tail that may be modeled by a generalized Lorentzian distribution. The maximum wave growth due to hot proton temperature anisotropy was found to occur for the parallel wave propagation.

Chaston et al. [1999] discussed the observations of electromagnetic bursts in the near-Earth magnetotail by ISEE 1 and ISEE 2. Since the frequency range of the observed waves contains the cyclotron frequencies of the ion components found in this region of space, they loosely term these bursts "electromagnetic ion-cyclotron waves." The polarized bursts are often accompanied by anisotropic ion distributions and/or significant field-aligned currents. The character of the polarized events is different than that of the largely unpolarized/incoherent activity. As reported by *Bauer et al.* [1995], the energetic spectrum of these bursts does not exhibit any structure near the ion gyrofrequencies. The measured wave amplitude of the bursty polarized activity may be significantly larger than that of the unpolarized activity over the same frequency band [*Chaston et al.*, 1999].

Several distribution functions of energetic electrons observed in the topside auroral ionosphere cannot result only from acceleration by a quasi-static electric potential drop, causing only a primary electron beam [*Lynch et al.*, 1994]. The bursts of downgoing, field-aligned electrons may be generated by waves and can subsequently generate other waves.

The term "broadband extremely low frequency (BB-ELF) waves" refers to the electric field fluctuations in the range 10 Hz to 3 kHz observed in the auroral ionosphere by sounding rockets and satellites at altitudes in the range 850–1700 km [*André et al.*, 1998; *Kintner et al.*, 1996]. It was found that these fluctuations are gyroresonant with the unheated ionospheric ion population. A comparison was made between space relevant observational signatures, such as frequency, spectra, phase velocities, excitation thresholds, and ion heating, and those signatures associated with EIC waves excited in a laboratory experiment [*Koepke et al.*, 1999]. It was concluded that the observed BB-ELF waves may be excited by a plasma instability related to inhomogeneity in the perpendicular plasma flow in the presence of parallel current.

This study considers the wave characteristics and generation mechanisms of both quasi-stationary electrostatic ion-cyclotron turbulence and bursts of polarized transverse electromagnetic waves at frequencies close to the proton gyrofrequency. The first purpose of this work is to investigate transport and energization of both the thermal and auroral plasma in the presence of quasi-stationary, current-driven EIC turbulence in the magnetosphere. In a self-consistent way, this is done numerically in dependence on the FAC intensity, the thickness of the turbulent region, and the intensities of the EIC waves and magnetospheric convection, respectively. Second, the dispersion relation of electromagnetic waves in anisotropic convecting plasma will be obtained. Third, the behavior of the wave vector and increment of wave growth will be estimated in dependence on the frequency and polarization of the waves.

2. Anomalous Transport of Thermal and Auroral Plasma in the Presence of Quasi-Stationary EIC Turbulence

A closed magnetic flux tube is given in the auroral magnetosphere. To describe this flux tube, the empirical model of the magnetospheric field presented by *Tsyganenko* [1995] is used. The behavior of the anisotropic plasma is described by the system of MHD equations. Additionally, the dispersion equation of the EIC waves [*Lominadze and Stepanov*, 1984] and an equation for the balance between growth and damping rates of the waves are taken into account. To describe anomalous transport of the thermal and auroral plasma, we use the model equations presented by *Zakharov and Meister* [1999].

In our model, the magnetospheric plasma consists of four components. They are the thermal protons ($j = 1$) and electrons ($j = 2$) as well as the auroral protons ($j = 3$) and electrons ($j = 4$). n_j, $\mathbf{v}_j$, $T_{\|j}$, and $T_{\perp j}$ designate particle density, mean velocity, and the parallel and perpendicular temperature components of the plasma, respectively. The plasma obeys the condition of quasi-neutrality

$$\sum_{j=1,4} q_j n_j = 0 \tag{1}$$

where q_j is the electric charge per particle.

The velocity equals $\mathbf{v}_j = \mathbf{v}_{\|j} + \mathbf{v}_{\perp j}$ where $\mathbf{v}_{\|j}$ and $\mathbf{v}_{\perp j}$ are the parallel and perpendicular components of $\mathbf{v}_j$, respectively. Taking the electric, curvature, and gradient drifts into account, $\mathbf{v}_{\perp j}$ may be approximated by [*Goldstone and Rutherford*, 1995]

$$\mathbf{v}_{\perp j} = \mathbf{v}_e + \mathbf{v}_{cj} + \mathbf{v}_{gj} = \frac{\mathbf{E}\times\mathbf{B}}{B^2}$$

$$+\frac{\mathbf{B}\times T_{\|j}(\mathbf{b}\nabla)\mathbf{b}}{q_j B^2} + \frac{\mathbf{B}\times T_{\perp j}\nabla B}{q_j B^3} \tag{2}$$

where $\mathbf{E}$ is the total strength of the electric field, $\mathbf{E} = \mathbf{E}_\| + \mathbf{E}_\perp$, $\mathbf{E}_\|$ and $\mathbf{E}_\perp$ are the parallel and perpendicular components of $\mathbf{E}$. $\mathbf{E}_\perp$ is caused by magnetospheric convection, $\mathbf{b}$ is the unit vector directed along the geomagnetic field $\mathbf{B}$.

The continuity and momentum equations of the anisotropic plasma are [*Goldstone and Rutherford*, 1995]

$$\frac{\partial n_j}{\partial t} + B\frac{\partial}{\partial s}\left(\frac{n_j v_{\|j}}{B}\right) = -\mathrm{div}_\perp(n_j \mathbf{v}_{\perp j}) \tag{3}$$

and

$$m_j n_j\left(\frac{\partial v_{\|j}}{\partial t} + v_{\|j}\frac{\partial v_{\|j}}{\partial s}\right)$$

$$= q_j n_j E_\| - (\nabla \mathbf{P}_j)_\| + R_{\|j} + F_{\|j} - m_j n_j(\mathbf{v}_{\perp j}\nabla)v_{\|j} \tag{4}$$

where $R_{\|j}$ and $F_{\|j}$ are the parallel components of the friction force caused by wave-particle interaction and of the gravitational force per unit of volume, respectively. T_j designates the effective temperature of the plasma defined by the expression $T_j = 2T_{\perp j}/3 + T_{\|j}/3$. Thus, one obtains

$$\begin{cases} T_{\|j} &= 3T_j\eta_j/(\eta_j+2) \\ T_{\perp j} &= 3T_j/(\eta_j+2) \end{cases} \tag{5}$$

where $\eta_j = T_{\|j}/T_{\perp j}$.

To calculate T_j, the following equation that describes the thermal balance of the plasma is used [*Goldstone and Rutherford*, 1995]

$$n_j\frac{\partial}{\partial t}\left(\frac{3}{2}k_B T_j\right) + n_j v_{\|j}\frac{\partial}{\partial s}\left(\frac{3}{2}k_B T_j\right)$$

$$+B\frac{\partial}{\partial s}\left(\frac{Q_{\|j}}{B}\right) + p_{\|j}\mathrm{div}(\mathbf{v}_{\|j})$$

$$= \gamma_j W - R_{\|j} v_{\|j}$$

$$-n_j(\mathbf{v}_{\perp j}\nabla)\left(\frac{3}{2}k_B T_j\right) - p_\perp \mathrm{div}(\mathbf{v}_{\perp j}) \tag{6}$$

where $Q_{\|j}$ is the thermal flux density caused by the thermal conductivity along $\mathbf{B}$, $Q_{\|j} = -k_{Tj}\partial(k_B T_j)/\partial s$, k_{Tj} is the coefficient of thermal conductivity, $k_{Tj} = 5n_j k_B T_j/(2m_j\nu_j)$, ν_j is the collision frequency of the particles scattered by the EIC waves, γ_j is the growth (or damping) rate of the EIC waves scattering the particles, W is the energy of the waves per unit of volume.

To apply the *Tsyganenko* [1995] model of the magnetospheric field, the geophysical conditions of equinox and moderate geomagnetic activity ($AE = 50$) are given. The solar-magnetic (SM) coordinate system (x, y, z) is used to describe the magnetic field [*Sergeev and Tsyganenko*, 1980]. The chosen magnetic field line intersects the equatorial plane of the magnetosphere at the point $A(x = -8, y = -6)$ where x and y are expressed in units of the Earth radius R_E. The length s along $\mathbf{B}$ is counted from the initial point located at the altitude $h = h_b = 1000$ km in the southern hemisphere. The given magnetic field line is situated inside a narrow flux tube; the radius of the cross-section may be estimated as $r_\perp(s) = [\Phi/(\pi B)]^{1/2}$ where Φ is the magnetic flux within this tube. The latter is filled with turbulent plasma. According to *Liperovsky and Pudovkin* [1983], satellite data averaged over the nightside auroral zone are used to describe the background plasma located outside the turbulent region.

For the system of equations (1)–(6), the initial value problem is considered. For each time step Δt, the difference scheme is applied based on the decomposition method [*Samarsky and Nikolaev*, 1978]. The algorithm of decomposition consists of four steps. At the first and second steps, only the effects of the plasma transport along $\mathbf{B}$ are considered. At the third step, only the effects of the plasma transport across $\mathbf{B}$ are simulated. At the fourth step, the effects of the EIC turbulence are additionally taken into account. To calculate the wave-dependent terms $R_{\|j}$ and $\gamma_j W$, additionally the dispersion equation of the EIC waves and the balance between growth and damping rates of the waves are taken into account. The dependence between the plasma and wave parameters is non-linear. Therefore, the iterations are performed to calculate the parameters of the plasma and of the EIC waves.

Figures 1–6 show the results of the numerical calculations obtained for the stationary state. There, profiles of the plasma parameters and of the parallel electric field versus the length s along the given magnetic field line are presented.

Figures 1, 2, and 3 are obtained for the density n_j, the temperature T_j, and for the parallel flux density $n_j v_{\|j}$ of the plasma, respectively. Figure 4 represents the profiles of the ratio between the potential and thermal energies per particle $q_j V/(k_B T_j)$ where V is the electric potential, $\mathbf{E} = -\nabla V$, and $V(s = 0) = 0$.

Figures 5 and 6 represent the profiles of the coefficient of thermal conductivity k_{Tj} and of the parallel electric field $E_\|$, respectively. In the latter case, both the total strength $E_\|$ and the contribution $-R_{\|2}/(q_2 n_2)$ due to the presence of the anomalous resistivity of the plasma are shown.

Profiles are presented for the plasma parameters and the parallel electric field along one and the same magnetic field line in both the southern and northern hemispheres. The given magnetic field line intersects the geomagnetic equatorial plane at $s = s_m \approx 11.2\ R_E$.

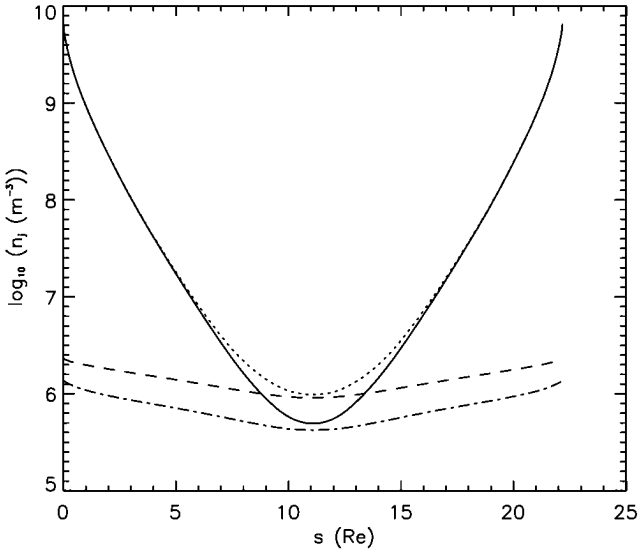

Figure 1. Profiles of the plasma density calculated for the stationary state versus the length of the magnetic field line given in the nightside auroral magnetosphere. The solid and dotted (dashed and dash-dot) lines are shown for the thermal (auroral) protons and electrons, respectively. The curves are shown for the case where $\Delta r_\perp = 100$ km, $E_\perp = 10$ mV m^{-1}, and $W/(nk_BT_2) = 1 \times 10^{-3}$ at $s = 0$. Besides, $n_1/n_3 = 10$ at the top of the given magnetic field line ($s = s_m$) for $t = 0$.

In our model, the value of the density of the electric current $j_{\|b}$ flowing from the magnetosphere into the ionosphere at $s = 0$ is not considered to be constant. Therefore, this value may be different in dependence on the choice of the model parameters. For Figure 1, the current density is found to be $j_{\|b} \approx 3.1 \times 10^{-6}$ A m^{-2}.

The maximum value ΔV_m of the parallel difference of the electric potential in one hemisphere (northern or southern) amounts to $\Delta V_m \approx 1.2$ kV.

The presence of the parallel electric field and the anomalous resistivity cause an energization of the plasma. Under present conditions, the thermal conductivity along **B** and the convection across **B** effectively prevent heating of

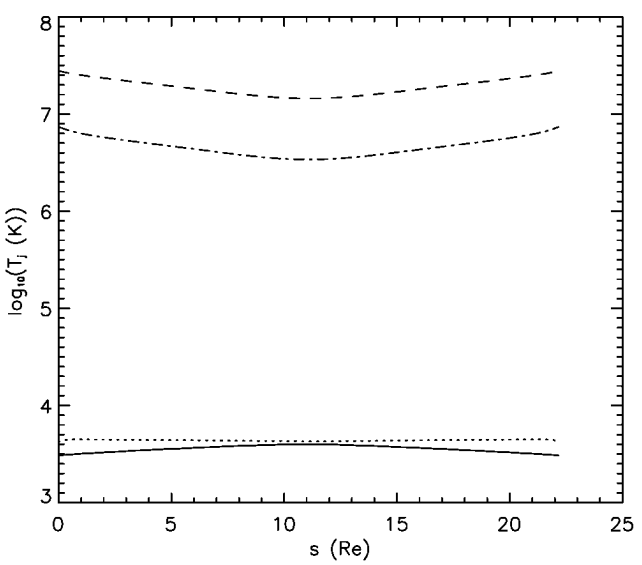

Figure 2. Same as Figure 1, but for the plasma temperature.

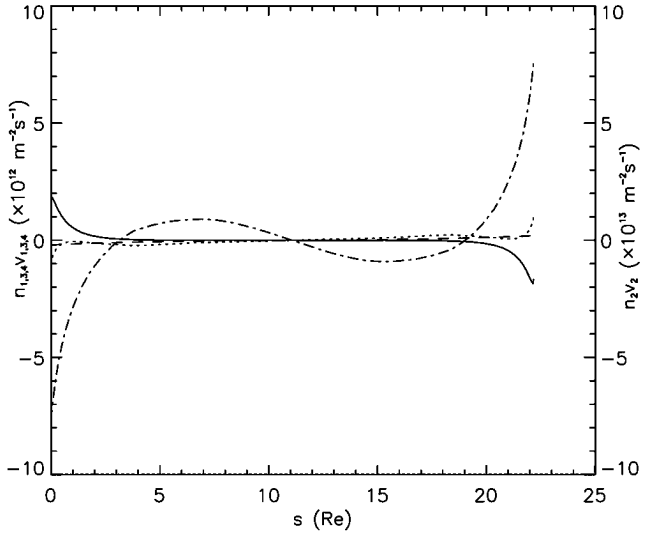

Figure 3. Same as Figure 1, but for the flux density of the plasma. The right-side scale is introduced for large fluxes of thermal electrons, the left-side scale is used for all other plasma components.

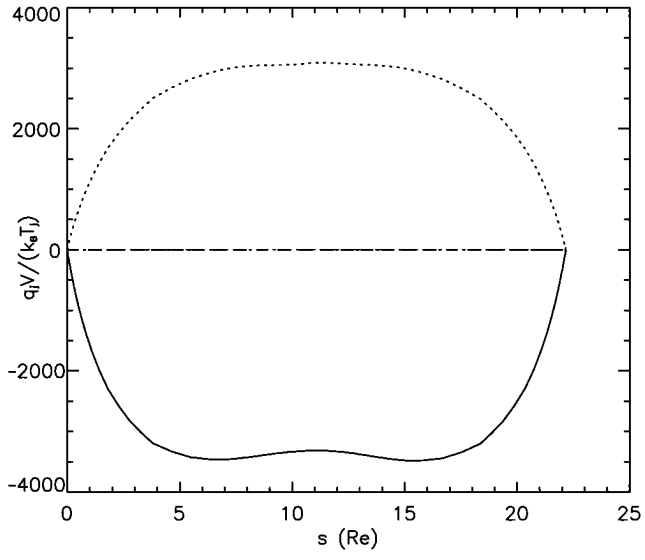

Figure 4. Same as Figure 1, but for the ratio between the potential and thermal energies per particle.

the thermal plasma. In our model, the anomalous thermal conductivity is absent in the auroral plasma as the wave-particle interaction is negligible for this component of the plasma. The pressure gradients of the auroral plasma along **B** increase while the intensity of the EIC waves becomes larger. The total flux density of the electrons directed from the magnetosphere into the ionosphere becomes larger while the strength of the upward-directed field $E_\parallel$ increases. Under the same conditions, the field-aligned fluxes carried by the electrons are much larger than those carried by the protons.

Figures 1–6 allows us to estimate how much the parallel electric field $E_\parallel$ may influence the profiles of n_j, $v_{\parallel j}$, and T_j. For the thermal plasma, this influence is expected to be much more intensive than for the auroral plasma. This is so because, with respect to the order of magnitude, the ratio $|q_j V/(k_B T_j)|$ may be equal to much larger values for $j = 1, 2$ than for $j = 3, 4$.

Due to magnetospheric convection, the colder (background) plasma flows into the given flux tube. Then, the heated plasma leaves this tube. The effectiveness of this loss depends strongly on the ratio of the difference of the electric potential across the tube to the magnetic flux Φ of the same tube. While the ratio mentioned above becomes smaller, the temperatures of both protons and electrons increase. After all, the thermal conductivity cannot prevent the plasma from intensive heating [*Zakharov and Meister*, 1999]. According to Figure 5, with respect to the order of magnitude, the coefficient of thermal conductivity of the electrons is about four orders larger than that of the protons. For that reason, the ratio T_1/T_2 rises [*Zakharov and Meister*, 1999]. In such a case, the absolute values of both the increment γ_1 and the decrement γ_2 of the EIC waves decrease. Thus, the EIC turbulence may be damped.

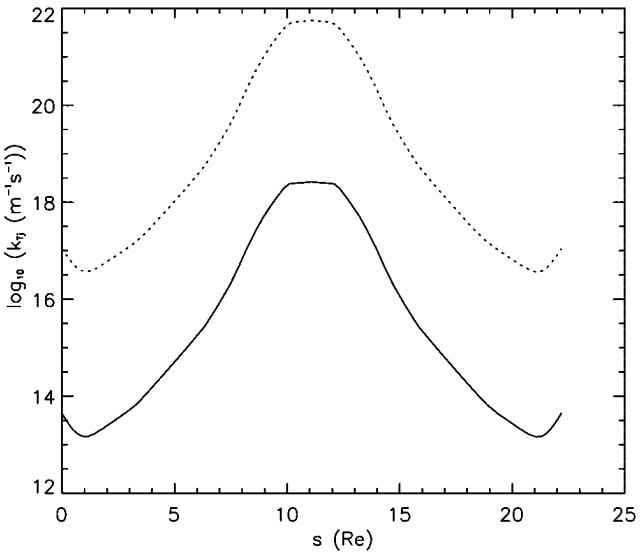

Figure 5. Profiles of the coefficient of thermal conductivity of plasma calculated for the stationary state versus the length of the magnetic field line given in the nightside auroral magnetosphere. The solid and dotted lines indicate thermal protons and electrons, respectively. The curves are shown for the case where $\Delta r_\perp = 100$ km, $E_\perp = 10$ mV m^{-1}, and $W/(nk_BT_2) = 10^{-3}$ at $s = 0$. Besides, $n_1/n_3 = 10$ at the top of the given magnetic field line ($s = s_m$) for $t = 0$.

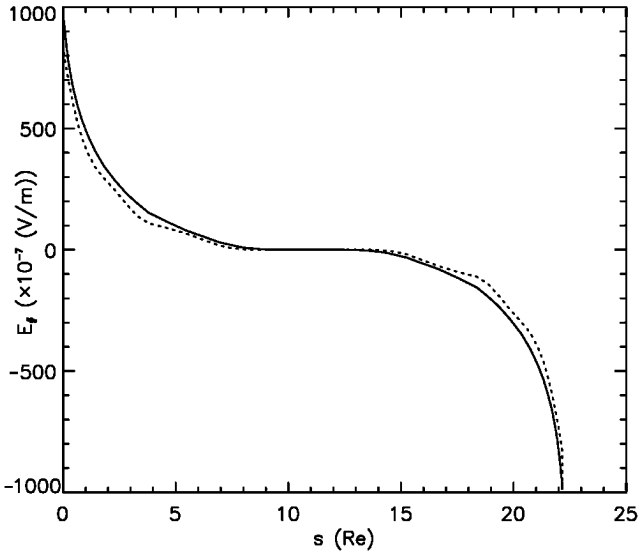

Figure 6. Profiles of the parallel electric field calculated for the stationary state versus the length of the magnetic field line given in the nightside auroral magnetosphere. The solid and dotted lines represent the strength of the total parallel electric field and the part of the parallel electric field caused by the anomalous resistivity of the plasma, respectively. The curves are shown for the case where $\Delta r_\perp = 100$ km, $E_\perp = 10$ mV m^{-1}, and $W/(nk_BT_2) = 1 \times 10^{-3}$ at $s = 0$. Besides, $n_1/n_3 = 10$ at the top of the given magnetic field line ($s = s_m$) for $t = 0$.

On the contrary, when the flux tube becomes narrower, the convective heat loss acts more effectively to prevent the plasma from intensive heating. This is the case to which Figures 1–6 are related.

The thermal conductivity of the plasma alone cannot prevent the thermal plasma from intensive heating in thick magnetic flux tubes when the convection is weak and the relative intensity of the EIC turbulence amounts to $W/(n_2k_BT_2) \geq 10^{-3}$ [*Zakharov and Meister*, 1999]. However, it may be that, besides the EIC turbulence, other mechanisms provide greater thermal conductivity.

As shown in Figure 5, the coefficient of thermal conductivity k_{Tj} ($j = 1, 2$) has its largest values at high altitudes, and it decreases when the observational point moves downward along **B**. This is so as the intensity of turbulence $W/(n_2k_BT_2)$ decreases while the observational point moves along **B** toward higher altitudes. Anomalous resistivity is only one factor causing the appearance of parallel electric fields in the auroral magnetosphere. In our model, these fields may also be caused by polarization of both the thermal and auroral plasma as well as by the presence of the component of the inertia force. Figure 6 shows that the total parallel electric field $E_\parallel$ is almost completely caused by

anomalous resistivity. When the observational point moves along **B** toward lower altitudes, the values of $E_\parallel$ driven by anomalous resistivity increase.

3. Modeling of Bursts of Obliquely Propagating EMIC Waves

The derivation of the general dielectric tensor **K** for obliquely propagating linear waves in a hot magnetized plasma has been carried out by many authors (e.g., *Krall and Trivelpiece* [1973]). General expressions for the elements of the dielectric tensor for an arbitrary particle distribution function are given by *Summers et al.* [1994]. *Xue et al.* [1996] adopted these expressions to describe EMIC waves in a plasma with temperature anisotropy. *Gary and Schriver* [1987] and *Summers and Thorne* [1992] worked out the dispersion relations for EMIC waves propagating along **B** in a drifting plasma with temperature anisotropy. *Gary and Schriver* [1987] ([*Summers and Thorne*, 1992]) supposed the distribution functions of the plasma components to be Maxwellian (Lorentzian).

In this section, the expressions evolved for **K** by *Gary and Schriver* [1987] and *Xue et al.* [1996] will be generalized. To do this, the effects of the plasma drift will be additionally taken into account for obliquely propagating waves.

We assume the plasma to be homogeneous, infinite, and immersed in a uniform magnetic field pointing in the z-direction of a Cartesian coordinate system. We assume further that perturbations about the zero-order values of the particle distribution function and the electric and magnetic fields are small, that all perturbed quantities vary as $e^{i(\mathbf{kr}-\omega' t)}$ where **k** is the wave vector, **r** is the radius-vector of the observational point, ω' is the complex frequency of electromagnetic oscillations, $\omega' = \omega + i\gamma$, γ is the wave growth (damping) rate when $\gamma > 0$ ($\gamma < 0$), and t is the time. Without loss of generality, the wave vector **k** may be written as

$$\mathbf{k} = k_\perp \mathbf{e}_x + k_\parallel \mathbf{e}_z \tag{7}$$

where $\mathbf{e}_x$ and $\mathbf{e}_z$ are the unit vectors of the coordinate system, which are directed along the x and z coordinate axes, respectively, $k_\perp$ and $k_\parallel$ are the components of **k**, which are perpendicular and parallel to **B**, respectively.

We consider the case where the mean velocities of all components of the plasma are directed along **B**. In particular, some of these velocities or all of them may be equal to zero.

By solving the Maxwell equations and the Vlasov equation, the following dispersion relation may be found for oblique waves in a hot magnetized plasma

$$F = An^4 + Dn^2 + C = 0 \tag{8}$$

where n is the refractive index, $n = ck/\omega'$, c is the velocity of light,

$$A = K_{xx}\sin^2\lambda + (K_{xz} + K_{zx})\sin\lambda\cos\lambda + K_{zz}\cos^2\lambda \tag{9}$$

λ is the angle between the wave vector **k** and the z (or magnetic field) direction,

$$D = K_{xz}K_{zx} - K_{xx}K_{zz} - AK_{yy} + K_{xy}(K_{yz} - K_{zy})\sin\lambda\cos\lambda - K_{xy}^2\sin^2\lambda + K_{yz}K_{zy}\cos^2\lambda \tag{10}$$

$$C = K_{yy}(K_{xx}K_{zz} - K_{xz}K_{zx}) + K_{xy}(K_{xy}K_{zz} + K_{yz}K_{zx} - K_{zy}K_{xz}) - K_{xx}K_{yz}\ K_{zy} \tag{11}$$

$K_{\alpha\beta}$ are the components of the dielectric tensor **K**, and $\alpha = \{x, y, z\}$, $\beta = \{x, y, z\}$.

The distribution of the convective anisotropic plasma may be described by a bi-Maxwellian function shifted along the mean magnetic field $\mathbf{B} = B\mathbf{e}_z$

$$f_\sigma = \frac{1}{\pi^{3/2}}\frac{1}{a_{\parallel\sigma}a_{\perp\sigma}^2}\exp\left(-\frac{(v_\parallel - v_{D\sigma})^2}{a_{\parallel\sigma}^2} - \frac{v_\perp^2}{a_{\perp\sigma}^2}\right) \tag{12}$$

where $a_{\parallel\sigma}$ and $a_{\perp\sigma}$ are the parallel and perpendicular thermal velocities of the plasma component σ, $a_{\perp,\parallel\sigma} = (2k_BT_{\perp,\parallel\sigma}/m_\sigma)^{1/2}$, and k_B is the Boltzmann constant.

We worked out that the components of the dielectric tensor $K_{\alpha\beta}$ may be expressed by

$$K_{xx} = 1 + \sum_\sigma \frac{\omega_{p\sigma}^2}{\omega'^2}\sum_{n=-\infty}^{\infty}\frac{n^2\Lambda_n}{\nu_\sigma}G_{n\sigma} \tag{13}$$

$$K_{xy} = \sum_\sigma \frac{\omega_{p\sigma}^2}{\omega'^2}\sum_{n=-\infty}^{\infty} in\Lambda_n' G_{n\sigma} \tag{14}$$

$$K_{yx} = -K_{xy} \tag{15}$$

$$K_{yy} = 1 + \sum_\sigma \frac{\omega_{p\sigma}^2}{\omega'^2}\sum_{n=-\infty}^{\infty}\frac{n^2\Lambda_n - 2\nu_\sigma^2\Lambda_n'}{\nu_\sigma}G_{n\sigma} \tag{16}$$

$$K_{xz} = \sum_\sigma \frac{\omega_{p\sigma}^2}{\omega'^2}\frac{a_{\parallel\sigma}}{a_{\perp\sigma}}\sum_{n=-\infty}^{\infty}\frac{\sqrt{2}n\Lambda_n\epsilon_\sigma}{\sqrt{\nu_\sigma}}H_{n\sigma} \tag{17}$$

$$K_{zx} = \sum_\sigma \frac{\omega_{p\sigma}^2}{\omega'^2}\frac{a_{\parallel\sigma}}{a_{\perp\sigma}}\sum_{n=-\infty}^{\infty}\frac{\sqrt{2}n\Lambda_n\epsilon_\sigma}{\sqrt{\nu_\sigma}}M_{n\sigma} \tag{18}$$

$$K_{yz} = \sum_\sigma \frac{\omega_{p\sigma}^2}{\omega'^2}\frac{a_{\parallel\sigma}}{a_{\perp\sigma}}\sum_{n=-\infty}^{\infty}(-\sqrt{2}i\epsilon_\sigma\sqrt{\nu_\sigma}\Lambda_n')H_{n\sigma} \tag{19}$$

$$K_{zy} = \sum_\sigma \frac{\omega_{p\sigma}^2}{\omega'^2}\frac{a_{\parallel\sigma}}{a_{\perp\sigma}}\sum_{n=-\infty}^{\infty}\sqrt{2}i\epsilon_\sigma\sqrt{\nu_\sigma}\Lambda_n' M_{n\sigma} \tag{20}$$

$$K_{zz} = 1 + \sum_\sigma \frac{\omega_{p\sigma}^2}{\omega'^2}\frac{a_{\parallel\sigma}}{a_{\perp\sigma}}\sum_{n=-\infty}^{\infty}2\Lambda_n\frac{a_{\parallel\sigma}}{a_{\perp\sigma}}N_{n\sigma} \tag{21}$$

where

$$G_{n\sigma} = A_\sigma^M(1+\eta_{n\sigma}^* Z(\eta_{n\sigma}^*)) + \frac{\omega'^*}{k_\parallel a_{\parallel\sigma}} Z(\eta_{n\sigma}^*)$$

$$H_{n\sigma} = (A_\sigma^M \eta_{n\sigma} + \frac{\omega'}{k_\parallel a_{\parallel\sigma}})(1+\eta_{n\sigma}^* Z(\eta_{n\sigma}^*))$$

$$+\frac{n\omega_{c\sigma} v_{D\sigma}}{k_\parallel a_{\parallel\sigma}^2} Z(\eta_{n\sigma}^*)$$

$$M_{n\sigma} = (A_\sigma^M \eta_{n\sigma} + \frac{\omega'}{k_\parallel a_{\parallel\sigma}})(1+\eta_{n\sigma}^* Z(\eta_{n\sigma}^*))$$

$$-\frac{v_{D\sigma}}{a_{\parallel\sigma}}(1+\eta_{n\sigma} Z(\eta_{n\sigma}^*))$$

$$N_{n\sigma} = (A_\sigma^M \eta_{n\sigma} + \frac{\omega'}{k_\parallel a_{\parallel\sigma}})(1+\eta_{n\sigma}^* Z(\eta_{n\sigma}^*))\eta_{n\sigma}$$

$$+\frac{n\omega_{c\sigma} v_{D\sigma}}{k_\parallel a_{\parallel\sigma}^2}(1+\eta_{n\sigma} Z(\eta_{n\sigma}^*))$$

$\omega_{p\sigma}$ is the plasma frequency, $\omega_{p\sigma} = [n_\sigma q_\sigma^2/(m_\sigma \varepsilon_0)]^{1/2}$, $\Lambda_n = \exp(-\nu_\sigma) I_n(\nu_\sigma)$, I_n is the modified Bessel function of the first kind of order n,

$$\Lambda_n' = \frac{\partial \Lambda_n}{\partial \nu_\sigma}$$

$$A_\sigma^M = \frac{a_{\perp\sigma}^2}{a_{\parallel\sigma}^2} - 1 = \frac{T_{\perp\sigma}}{T_{\parallel\sigma}} - 1$$

$$\omega'^* = \omega' - k_\parallel v_{D\sigma}$$

$$\eta_{n\sigma} = \frac{\omega' - n\omega_{c\sigma}}{k_\parallel a_{\parallel\sigma}}$$

$$\eta_{n\sigma}^* = \frac{\omega' - k_\parallel v_{D\sigma} - n\omega_{c\sigma}}{k_\parallel a_{\parallel\sigma}}$$

$$\nu_\sigma = \frac{k_\perp^2 a_{\perp\sigma}^2}{2\omega_{c\sigma}^2}$$

Z is the plasma dispersion function [*Summers et al.*, 1994], σ denotes the plasma component, m_σ and q_σ are the mass and electric charge per particle, respectively, n_σ is the partial density of the plasma, ε_0 is the dielectric susceptibility of the vacuum, $v_\parallel$ and $v_\perp$ are the parallel and perpendicular components of the total velocity $\mathbf{v}$ of a charged particle with respect to $\mathbf{B}$, respectively, $\omega_{c\sigma}$ is the gyrofrequency of a charged particle of the kind σ, and $\omega_{c\sigma} = q_\sigma B/m_\sigma$, $a_{\parallel\sigma}$ and $a_{\perp\sigma}$ are the parallel and perpendicular thermal velocities of the plasma component σ, $a_{\perp,\parallel\sigma} = (2k_B T_{\perp,\parallel\sigma}/m_\sigma)^{1/2}$, and k_B is the Boltzmann constant.

In the case where $v_{D\sigma} = 0$, the expressions (13)–(21) obtained by us for the components of the dielectric tensor $\mathbf{K}$ correspond to those presented by *Xue et al.* [1996].

Xue et al. [1996] investigated the dispersive properties of the EMIC oblique waves below the proton gyrofrequency ω_{c1}, which are excited due to the temperature anisotropy of energetic protons near the geomagnetic equator at $L = 7$ in the plasma sheet. The effects of plasma drift were not taken into account. It was found that the EMIC waves may indeed be unstable under these conditions. The maximum values of the wave growth rate normalized by the proton gyrofrequency were estimated to be of the order of $\gamma/\omega_{c1} \approx 10^{-2}$.

Chaston et al. [1999] considered EMIC waves propagating along $\mathbf{B}$ ($\mathbf{k}\times\mathbf{B} = 0$) in the drifting plasma of the near-Earth magnetotail. They showed that the influence of heavy ions on wave growth and dispersion in the region of instability may be ignored. They also demonstrated that the properties of the instability remain almost the same as in the case $\mathbf{k}\times\mathbf{B} = 0$ if the angle between the wave vector $\mathbf{k}$ and the direction of the main magnetic field $\mathbf{B}$ is less than 45°. Taking the effects of the plasma drift into account and solving the dispersion relation of the EMIC waves, *Chaston et al.* [1999] estimated the maximum values of γ/ω_{c1} to be of the order of 10^{-1}.

In this study, we investigate the growth and dispersion properties of oblique ion-cyclotron waves with frequencies close to the proton gyrofrequency. In the case where $|\gamma/\omega_{c1}| \ll 1$, the dispersion relation (8) may be approximated by

$$\mathrm{Re}\ F(\omega) = 0 \tag{22}$$

$$\gamma = -\frac{\mathrm{Im}\ F(\omega)}{\frac{\partial \mathrm{Re}\ F(\omega)}{\partial \omega}} \tag{23}$$

The expressions (13)–(21) obtained for the components $K_{\alpha\beta}$ of the dielectric tensor $\mathbf{K}$ are employed in (22) and (23). The approximate dispersion relation (22) is solved numerically using the trial method [*Korn and Korn*, 1968]. To calculate the perpendicular component $k_\perp$ of the wave vector $\mathbf{k}$, we specify the (real) values for the wave frequency ω and the parallel component $k_\parallel$ of the wave vector. Then, the wave growth (or damping) rate γ is calculated from (23).

The results of the numerical calculations are shown in Figure 7. Of course, the results depend on the choices of the concrete plasma parameters (which are given in the figure caption). In Figure 7, the curves are related to the right-hand polarized ion-cyclotron waves with frequencies above the proton gyrofrequency.

The numerical estimates show that the contributions of thermal plasma to the components of the dielectric tensor $\mathbf{K}$ are about two orders of magnitude larger than the contributions of the energetic plasma. For that reason, the parameters are given only for the thermal plasma. To guarantee the validity of (23), the calculations are only performed for the narrow frequency bands close to the proton gyrofrequency, for which $|\gamma/\omega_{c1}| < 1$.

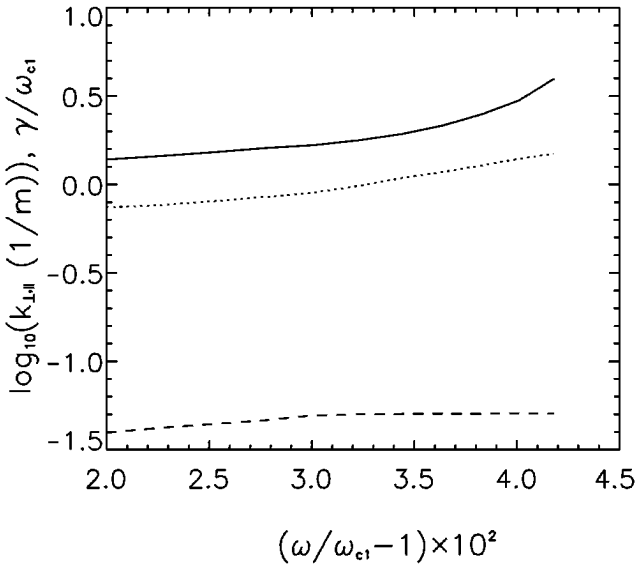

Figure 7. Frequency dependencies of the growth rate γ (solid line) and of the components of the wave number perpendicular $k_\perp$ (dotted line) and parallel $k_\parallel$ (dashed line). The curves are shown for an altitude of $h = 1050$ km, the magnetospheric field induction $B = 3.6 \times 10^4$ nT, the temperatures, densities, and main velocities of thermal protons and electrons $T_1 = 3.0 \times 10^3$ K, $T_2 = 4.1 \times 10^3$ K, $n_1 \approx n_2 = 6.4 \times 10^9$ m^{-3}, $v_{D1} = 2.3 \times 10^2$ m s^{-1}, and $v_{D2} = -1.6 \times 10^3$ m s^{-1}, respectively, in the southern hemisphere at the given magnetospheric field line.

In the case of our calculations, the FAC intensity amounts to $j_\parallel = 2.0 \times 10^{-6}$ A m^{-2}. The curves shown in Figure 7 are related to highly oblique ion-cyclotron waves. The analysis showed that the plasma instability is excited at lower values of the wave number k if the FAC intensity becomes larger. On the order of magnitude, the values of γ calculated by us correspond to those obtained for the drifting plasma of the near-Earth tail by *Chaston et al.* [1999]. On the other hand, *Xue et al.* [1996] obtained that the maximum wave growth due to hot proton temperature anisotropy near the geomagnetic equator at $L = 7$ is less by one to two orders of magnitude than that described here.

Repeating the calculations for a different choice of the observational point at the given magnetic field line, we find that the plasma instability in the drifting magnetospheric plasma is not localized at small altitudes ($h \approx 1000$ km). Instead, the region of plasma instability stretches to higher altitudes in the auroral magnetosphere. Besides, we can conclude that the plasma instability is excited at lower values of the wave number k if the altitude becomes larger.

It should be pointed out that numerical calculations were performed by us not only for the right-hand, but also for the left-hand polarized ion-cyclotron waves ($\omega < -\omega_{c1}$). It is found that the latter waves are also unstable under present conditions. On the order of magnitude, the growth rate of the left-hand polarized waves may reach the same values as were obtained above for the right-hand polarized waves.

4. Conclusions

A numerical solution of equations describing the anomalous transport of anisotropic magnetized plasma is found, and profiles of the parameters of the multi-component plasma and of the parallel electric field along the magnetospheric field are considered.

Having solved the stationary system of equations in a previous paper [*Zakharov and Meister*, 1999], the relaxation of the turbulent plasma and of the parallel electric fields and currents from an initial state up to the stationary state are simulated numerically. Thus, it is shown that stationary solutions indeed exist. In this context, acceleration and heating are considered, comparing the parameters of the turbulent plasma with those related to the background plasma in the neighborhood of the turbulent region.

The analysis shows that the current-driven EIC turbulence may cause the large-scale anomalous resistivity of the plasma of the Earth's ionosphere. The resonant wave-particle interaction is most effective for the upward-directed FAC with a density of a few 10^{-6} A m^{-2} at the upper boundary of the nightside auroral ionosphere ($h = 1000$ km). As shown, anomalous resistivity is able to produce differences of the electric potential along $\mathbf{B}$ in one (northern or southern) hemisphere of about a few kV.

The electron thermal conductivity is calculated to be about three to four orders of magnitude larger than the proton thermal conductivity. Electron thermal conductivity increases with altitude.

According to the results of numerical calculations presented by *Zakharov and Meister* [1999], magnetospheric convection and thermal conductivity are found to be the effective mechanisms providing the heat loss from the turbulent region. In the case of narrow magnetic flux tubes and intensive magnetospheric convection, these mechanisms effectively prevent the turbulent plasma from heating. In the case of thick magnetic flux tubes and weak convection, the current-driven anomalous resistivity results in significant heating of the plasma. The ratio between the temperatures of protons and electrons increases while the plasma is heated.

What is the relevance of the stationary solution in the sense of physics? As is well known, within MHDs, FAC disturbances are carried along the magnetic field lines by Alfvén waves. The time of propagation of Alfvén waves from the magnetosphere into the ionosphere depends on the geophysical conditions and, according to the estimates, may be of the order of a few minutes. This is much less than the duration of a typical magnetospheric substorm when intensive FACs evolve. The presence of intensive FACs may cause turbulence in the plasma. As is known from satellite experiments, electromagnetic noise is permanently observed in the magnetosphere as a large-scale phenomenon. Besides, small-scale bursts of electromagnetic noise are also observed. It is obvious that the bursts correspond to an unstable plasma. During bursts, the growth rate of electromagnetic noise may be significantly higher than its damping rate. Under such conditions, one has to deal with a nonequilibrium state and, particularly, temperature anisotropy may occur.

Thus, the growth and dispersion properties of oblique

ion-cyclotron waves excited in a drifting magnetized plasma are also investigated. The expressions evolved for the components $K_{\alpha\beta}$ of the dielectric tensor **K** of the anisotropic plasma by *Gary and Schriver* [1987] and *Xue et al.* [1996] are generalized. To do this, the effects of the plasma drift are also taken into account for obliquely propagating waves.

The approximate dispersion relation (22) is solved numerically for the geophysical conditions relevant to the region of intensive FAC of the auroral magnetosphere. The wave growth (or damping) rate γ is calculated from (23). It is found that the excited oblique ion-cyclotron waves may reveal the properties of bursts of polarized transverse electromagnetic waves at frequencies near the proton gyrofrequency. The curves shown in Figure 7 are related to highly oblique ion-cyclotron waves.

The resonant character of interactions of charged particles via ion-cyclotron waves is confirmed by the calculated dependence of the wave growth rate γ on the intensity of FAC. On the order of magnitude, the values of the wave growth rate γ calculated by us correspond to those obtained for the drifting plasma of the near-Earth tail by *Chaston et al.* [1999]. On the other hand, *Xue et al.* [1996] found that the maximum wave growth due to the hot proton temperature anisotropy near the geomagnetic equator at $L = 7$ is less by one to two orders of magnitude than that calculated by us.

An extended but not localized region of the plasma instability is found by numerical calculations; it stretches in the auroral magnetosphere. The plasma instability is excited at lower values of the wave number k if the altitude becomes larger.

Acknowledgment. V.E.Z. thanks the Gottlieb Daimler and Karl Benz Foundation for financing his stay at the Potsdam Astrophysical Institute to work on the given topic. C.-V.M. gratefully acknowledges financial support from project 24-04/055-2000 of the Ministerium für Wissenschaft, Forschung und Kultur des Landes Brandenburg, and from project ME 1207/7 of the Deutsche Forschungsgemeinschaft.

References

André, M., H. Koskinen, G. Gustafsson, and R. Lundin, Ion waves and upgoing ion beams observed by the Viking satellite, *Geophys. Res. Lett., 14*, 463, 1987.

André, M., P. Norqvist, L. Anderson, L. Eliasson, A. I. Eliasson, L. Blomberg, R. E. Erlandson, and J. Waldemark, Ion energization mechanisms at 1700 km in the auroral region, *J. Geophys. Res., 103*, 4199, 1998.

Bauer, T. M., W. Baumjohann, R. A. Treumann, N. Sckopke, and H. Lühr, Low frequency waves in the near-Earth plasma sheet, *J. Geophys. Res., 100*, 9605, 1995.

Block, L. P., Double layers, in *Physics of the Hot Plasma in the Magnetosphere*, edited by B. Hultqvist and L. Stenflo, p. 229, Plenum Press, New York, 1975.

Block, L. P., and C.-G. Fälthammar, Characteristics of magnetic field-aligned electric fields in the auroral acceleration region, in *Auroral Physics*, edited by C.-I. Meng, M. I. Rycroft, and L. A. Frank, p. 109, Cambridge University Press, New York, 1991.

Chaston, C. C., Y. D. Hu, and B. J. Fraser, Electromagnetic ion-cyclotron waves in the near-Earth magnetotail, *J. Geophys. Res., 104*, 6953, 1999.

Chiu, T. T., and J. M. Cornwall, Electrostatic model of a quiet auroral arc, *J. Geophys. Res, 85*, 543, 1980.

Chust, T. R., P. Louarn, M. Volwerk, H. de Feraudy, J.-E. Wahlund, and B. Holback, Electric fields with a large parallel component observed by the Freja spacecraft: Artifacts or real signals, *J. Geophys. Res., 103*, 215, 1998.

Erlandson, R. E., L. J. Zanetti, M. H. Acunã, A. I. Eriksson, L. Eliasson, M. H. Boehm, and L. G. Blomberg, Freja observations of electromagnetic ion-cyclotron ELF waves and transverse oxygen ion acceleration on auroral field lines, *Geophys. Res. Lett., 21*, 1855, 1994.

Gary, S. P., and D. Schriver, The electromagnetic ion-cyclotron beam anisotropy instability, *Planet. Space Sci., 35*, 51, 1987.

Goldstone, R. J., and P.-H. Rutherford, *Introduction to Plasma Physics*, Institute of Physics Publishing, Bristol, 1995.

Gorney, D. J., Potential structures and particle acceleration on auroral field lines, *Adv. Space Res., 4*, 499, 1984.

Hesse, M., J. Birn, and K. Schindler, A self-consistent two-dimensional resistive fluid theory of field-aligned potential structures including charge separation and magnetic and velocity shear, *J. Geophys. Res., 95*, 18,929, 1990.

Kindel, J. M., and C. F. Kennel, Topside current instabilities, *J. Geophys. Res., 76*, 3055, 1971.

Kintner, P. M., J. Bonnell, R. Arnoldy, K. Lynch, C. Pollock, and T. Moore, Transverse ion acceleration and plasma waves, *Geophys. Res. Lett., 23*, 1873, 1996.

Koepke, M. E., J. J. Carroll, and M. M. Zintl, Laboratory simulation of broadband ELF waves in the auroral ionosphere, *J. Geophys. Res., 104*, 14,397, 1999.

Korn, G. A., and T. K. Korn, *Mathematical Handbook*, McGraw-Hill, New York, 1968.

Krall, N. A., and A. W. Trivelpiece, *Principles of Plasma Physics*, McGraw-Hill, New York, 1973.

Liperovsky, V. A., and M. I. Pudovkin, *Anomalous Resistivity and Double Layers in the Magnetospheric Plasma (in Russian)*, pp. 122–146, Nauka, Moscow, 1983.

Lominadze, D. G., and K. N. Stepanov, Excitation of the low-frequency longitudinal oscillations in the magnetized plasma, *J. Theor. Phys. (in Russian), 34*, 1823, 1984.

Lund, E. J., and J. LaBelle, On the generation and propagation of auroral electromagnetic ion-cyclotron waves, *J. Geophys. Res., 102*, 17,241, 1997.

Lynch, K. A., R. L. Arnoldy, P. M. Kintner, and J. L. Vago, Electron distribution function behavior during localized transverse ion acceleration events in the topside ionosphere, *J. Geophys. Res., 99*, 2227, 1994.

Lysak, R. L., and T. Dum, Dynamics of magnetosphere-ionosphere coupling including turbulent transport, *J. Geophys. Res., 88*, 365, 1983.

Oscarsson, T., A. Vaivads, K. Rönnmark, J. H. Clemmons, H. de Feraudy, and B. Holback, Toward a consistent picture of the generation of electromagnetic ion-cyclotron ELF waves on auroral field lines, *J. Geophys. Res., 102*, 24,369, 1997.

Reiff, P. H., H. L. Collin, J. D. Craven, J. L. Burch, J. D. Winningham, E. G. Shelley, L. A. Frank, and M. A. Friedman, Determination of auroral electrostatic potentials using high- and low-altitude particle distributions, *J. Geophys. Res., 93*, 7441, 1988.

Reiff, P. H., G. Lu, J. H. Burch, J. D. Winningham, L. A. Frank, J. D. Craven, W. K. Peterson, and R. A. Heelis, On the high- and low-altitude limits of the auroral electric field region, in *Auroral Plasma Dynamics*, Geophys. Monogr. Ser., vol. 80, edited by R. L. Lysak, p. 143, AGU, Washington, D.C., 1993.

Sergeev, V. A., and N. A. Tsyganenko, *The Earth's Magnetosphere (in Russian)*, Nauka, Moscow, 1980.

Samarsky, A. A., and E. C. Nikolaev, *Integration Methods for the Grid Equations (in Russian)*, Nauka, Moscow, 1978.

Summers, D., and R. M. Thorne, A new tool for analyzing

microinstabilities in space plasmas modeled by a generalized Lorentzian (Kappa) distribution, *J. Geophys. Res., 97*, 16,827, 1992.

Summers, D., S. Xue, and R. M. Thorne, Calculation of the dielectric tensor for a generalized Lorentzian (kappa) distribution function, *Phys. Plasmas, 1*, 2012, 1994.

Temerin, M., C. Carlson, and J. P. McFadden, The acceleration of electrons by electromagnetic ion-cyclotron waves, in *Auroral Plasma Dynamics*, Geophys. Monogr. Ser., vol. 80, edited by R. L. Lysak, pp. 155–167, AGU, Washington, D.C., 1993.

Tsyganenko, N. A., Modeling the Earth's magnetospheric magnetic field confined within a realistic magnetopause, *J. Geophys. Res., 100*, 5599, 1995.

Xue, S., R. M. Thorne, and D. Summers, Growth and damping of oblique electromagnetic ion-cyclotron waves in the Earth's magnetosphere, *J. Geophys. Res., 101*, 15,457, 1996.

Zakharov, V. E., and C.-V. Meister, Current-driven plasma turbulence in a magnetic flux tube, *Astron. Nachr., 320*, 425, 1999.

V. E. Zakharov, Kaliningrad State University, Department of Physics, Kaliningrad 236032, Russia. (icid0087@soros.albertina.ru)

C.-V. Meister, Astrophysical Institute, Potsdam 14482, Germany. (cvmeister@aip.de)

(Received 1 September 2001; accepted 5 November 2002)